

BRIEF COMMUNICATION

Three-dimensional surface scanning methods in osteology: A topographical and geometric morphometric comparison

Lukas Waltenberger^{1,2}  | Katharina Rebay-Salisbury¹ | Philipp Mitteroecker²¹Austrian Archaeological Institute, Austrian Academy of Sciences, Vienna, Austria²Department of Evolutionary Biology, University of Vienna, Vienna, Austria**Correspondence**

Lukas Waltenberger, Institute for Oriental and European Archaeology, Austrian Academy of Sciences, Hollandstraße 11-13, 1020 Vienna, Austria.

Email: lukas.waltenberger@oeaw.ac.at

Funding information

H2020 European Research Council, Grant/Award Number: 676828

Abstract

Objectives: Three-dimensional (3D) data collected by structured light scanners, photogrammetry, and computed tomography (CT) scans are increasingly combined in joint analyses, even though the scanning techniques and reconstruction software differ considerably. The aim of the present study was to compare the quality and accuracy of surface models and landmark data obtained from modern clinical CT scanning, 3D structured light scanner, photogrammetry, and MicroScribe digitizer.

Material and methods: We tested 13 different photogrammetric software tools and compared surface models obtained by different methods for four articulated human pelvises in a topographical analysis. We also measured a set of 219 landmarks and semilandmarks twice on every surface as well as directly on the dry bones with a MicroScribe digitizer.

Results: Only one photogrammetric software package yielded surface models of the complete pelvises that could be used for further analysis. Despite the complex pelvic anatomy, all three methods (CT scanning, 3D structured light scanning, photogrammetry) yielded similar surface representations with average deviations among the surface models between 100 and 200 μm . A geometric morphometric analysis of the measured landmarks showed that the different scanning methods yielded similar shape variables, but data acquisition via MicroScribe digitizer was most prone to error.

Discussion: We demonstrated that three-dimensional models obtained by different methods can be combined in a single analysis. Photogrammetry proved to be a cheap, quick, and accurate method to generate 3D surface models at useful resolutions, but photogrammetry software packages differ enormously in quality.

KEYWORDS

3D structured light surface scanner, CT scanning, human pelvis, MicroScribe digitizer, photogrammetry

1 | INTRODUCTION

In the last decades, three-dimensional (3D) surface models have become increasingly important for geometric morphometric studies in

anthropology, bioarchaeology, and forensics. 3D surface representations can be easily shared (e.g., in online data repositories) and enable qualitative morphological assessments as well as morphometric measurements without interfering with the potentially fragile or precious original objects.

This is an open access article under the terms of the Creative Commons Attribution-NonCommercial-NoDerivs License, which permits use and distribution in any medium, provided the original work is properly cited, the use is non-commercial and no modifications or adaptations are made.

© 2021 The Authors. *American Journal of Physical Anthropology* published by Wiley Periodicals LLC.

Three methods are commonly used to produce 3D surface data: Surface scanning, photogrammetry, and computed tomography (CT) scanning, the latter of which is the only method that also yields information on internal structures. Geometric accuracy and spatial resolution of the digital surface model is key to further morphometric analysis.

2 | 3D SURFACE SCANNING

Surface scanners emit laser or visible light to survey the surface of an object. Light scanners provide colors and a sufficient resolution to measure distances or to place landmarks on human bones. Laser beams produce fewer errors in the surface mesh and are less problematic in daylight; however, no texture information is collected (Friess, 2012). Many scanners are lightweight, handheld, and portable (Adams et al., 2015).

Most surface scanners utilize the principle of triangulation to estimate a point cloud and to calculate a polygon mesh. Shaded areas, undercuts, and narrow structures that are outside the triangulation angle cannot be represented well in the 3D model (Friess, 2012). Hair, reflective surfaces, sharp edges, small holes, and translucent materials as well as dark or black-colored materials are also difficult to scan. Surface scanning has been successfully employed in osteology and anthropology (e.g., Hennessy & Stringer, 2002; Motani, 2005; Niven et al., 2009; Sholts et al., 2010; Tocheri et al., 2005; Windhager et al., 2019), medicine (e.g., Da Silveira et al., 2003; Kau et al., 2005; Kovacs et al., 2006; Toma et al., 2009; Yamada et al., 2002) and archaeology (e.g., Counts et al., 2016; Godin et al., 2002; Grosman et al., 2008; Kuzminsky & Gardiner, 2012; Wachowiak & Karas, 2009).

3 | PHOTOGRAMMETRY

Photogrammetry reconstructs the shape, color, and texture of the surface of objects from multiple pictures (Kraus, 2007) using a least-squares algorithm (Evin et al., 2016; Rütger et al., 2012). Since the beginning of digital photogrammetry, the processing algorithms have continuously improved and the resolution has increased from several millimeters (Faig, 1981; Lichti et al., 2002) to a few micrometers (González et al., 2015; Rütger et al., 2012). Nowadays it is an accurate, precise, and cheap technique (Munoz-Munoz et al., 2016). Photogrammetry has been applied in several research fields, ranging from anthropology (e.g., Adams et al., 2015; Fourie et al., 2011; Geoghegan, 1953; Ghoddousi et al., 2007; Martin & Knußmann, 1988), archaeology (e.g., Bouby et al., 2013; Counts et al., 2016; Grosman et al., 2008; Haukaas & Hodgetts, 2016; Porter et al., 2016), medicine (e.g., Aldridge et al., 2005; Grant et al., 2019; Jayaratne et al., 2009; Plooij et al., 2009), and geomorphology (e.g., Heritage et al., 1998; Lane et al., 1996; Nunez et al., 2013; Sapirstein, 2016; Verhoeven et al., 2012) to zoology (e.g., Breuer et al., 2007; Evin et al., 2016; Jaquet, 2006; Munoz-Munoz et al., 2016; Shrader et al., 2006).

In contrast to 3D surface scanners, which are calibrated and provide both shape and size information of the object, most photogrammetric methods capture only shape information unless the mesh is

manually calibrated based on a scale (e.g., measurement tape) placed next to the object (González et al., 2015). Including metadata of the internal geometry of the camera used to take the pictures (focal length, focal ratio, lens distortion, etc.) helps to scale the model accurately.

4 | CT SCANNING

CT scanning is a method to produce volumetric data from X-ray images taken from different angles. It allows one to investigate both internal and external structures of objects and, hence, is most useful for hidden and internal structures, such as bones in mummies, cremated remains in urns, trabecular bone structure, or endocranial morphology. Clinical CTs produce a stack of images with a spatial resolution of maximal 0.5 mm. In contrast to clinical CTs, in micro CT the distance between sample and emitter can be altered, and resolutions up to 1 μm or even less are possible, depending on the object's size and the field of view (Metscher, 2009; Rutty et al., 2013). However, not all objects are suitable for CT scanning: X-ray emission may harm living individuals or require fixation of the subject (Littlefield et al., 2004). Furthermore, the boundary between bone and air is not sharply depicted in CT scans (Hoffmann et al., 1979). This so-called partial volume effect and the limited resolution make CT scanning not optimal for creating 3D surface models (Littlefield et al., 2004). CT scanning is a time-consuming and costly method. Nonetheless, it has been used in numerous anthropological studies, especially on cranial and endocranial morphology (e.g., Coquerelle et al., 2013; Lloyd et al., 2016; Marcus et al., 2008; Neubauer et al., 2020).

5 | MICROSCRIBE DIGITIZER

In comparison to surface-based methods, a point MicroScribe digitizer is a quick and cheap method to collect small to intermediate sets of landmarks (Vu et al., 2017). It has been used in various fields, including anthropology and primatology (e.g., Aung et al., 1995; Cardini & Elton, 2008; Mehta & Marinescu, 2001; Mitteroecker et al., 2004; O'Higgins & Jones, 1998; Ross & Williams, 2008; Sholts et al., 2011; Singleton, 2002; Vidarsdottir et al., 2002; Von Cramon-Taubadel et al., 2007), medicine (e.g., Chen et al., 2008; Dastane et al., 1996), and zoology (e.g., Loy et al., 2011; Milne et al., 2009; Owen et al., 2014).

MicroScribe digitization is a tactile method using a stylus tip mounted on a mobile articulated sensor arm to capture the 3D coordinates of landmark points. Moving the stylus over the entire surface of an object, it is even possible to create a simple surface mesh with a MicroScribe digitizer (Mehta & Marinescu, 2001; Mitteroecker et al., 2004). However, a MicroScribe digitizer just collects the raw landmark coordinates, without any further surface information, which can make this method prone to error (e.g., missing or incorrectly ordered landmarks) as the collected data cannot be immediately checked before data analysis (Algee-Hewitt & Wheat, 2016; Menéndez, 2016). In most cases, the quality of the surface mesh and the precision of placed landmarks depend on the complexity and size of the studied object (Boldt et al., 2009).

Boldt et al. (2009) and Stephen et al. (2015) reported standard deviations of repeated MicroScribe measures of 0.1 mm. In contrast to the soft tissue model in Boldt et al. (2009), Stephen et al. (2015) used a technical reference model of stairs with clear edges and rectangular corners as landmark positions, which may underestimate the repeatability of anatomical landmarks (Aung et al., 1995; Van Vlijmen et al., 2011).

6 | COMPARISON OF METHODS

Several studies compared the performance of 3D surface scanner models to CT scanning (Adams et al., 2015; Evin et al., 2016; Fourie et al., 2011; Grant et al., 2019; Katz & Friess, 2014; Weinberg et al., 2006). Adams et al. (2015) compared surface meshes of hominin holotypes obtained by the Artec spider surface scanner, clinical CT and micro CT and reported mean surface deviations of 0.4 mm between the methods. The mesh gained by the surface scanner was slightly smaller in comparison with CT scanning. Katz and Friess (2014) and Fourie et al. (2011) found that the differences in landmark configurations set on meshes gained by surface scanning and photogrammetry on human faces and cranial surfaces varied less than the differences between individuals. Furthermore, Katz and Friess observed that photogrammetry produced slightly larger meshes than surface scanning. Similarly, Evin et al. (2016) detected a mean deviation of 90 μm between meshes obtained by photogrammetry and surface scanner as well as only small shape differences between landmark sets placed on these meshes. Contrarily, Grant et al. (2019) and Weinberg et al. (2006) measured surface deviations of 1.5 mm and 0.9 mm, respectively, between photogrammetry and surface scanning on soft tissue casts. However, in this rapidly evolving field, new photogrammetric software is developed and previous methods are updated. More recent publications demonstrate that photogrammetry has improved dramatically due to advanced algorithms and better cameras (González et al., 2015; Rütther et al., 2012). Within a decade, the number of available software increased from a handful to hundreds of products for different purposes. These software solutions differ dramatically in performance, resolution and reliability (see below).

Overall, the literature reveals a trend toward an increased accuracy in 3D surface scanning and photogrammetry from measurement errors higher than 1 mm (Kovacs et al., 2006; Kusnoto & Evans, 2002; Lichti et al., 2002; Marmulla et al., 2003) down to a few micrometers (Adams et al., 2015; Evin et al., 2016; Ghoddousi et al., 2007; Grant et al., 2019; Rütther et al., 2012). Similarly, many previous studies on the comparison of landmark configurations across different surface types focused on software that is not supported by the developers any more (e.g., Evin et al., 2016; Hassett & Lewis-Bale, 2017) or updated to newer versions with additional features, that should help the end-user to handle surface scanning and photogrammetry more easily and decrease surface errors (e.g., Friess, 2012; Katz & Friess, 2014; Munoz-Munoz et al., 2016). Despite a higher error rate of a MicroScribe digitizer in contrast to volume- or surface-based

methods (Algee-Hewitt & Wheat, 2016; Menéndez, 2016), all studies concluded that differences among datasets captured by different scanning methods are small enough to combine data from different sources. However, most of these earlier studies compared only two methods by using linear distances or landmark configurations.

The aim of the present study was to compare 13 different photogrammetry software packages to modern clinical CT scanning, 3D structured light scanner, and the MicroScribe digitizer by combining a comprehensive geometric morphometric analysis with a complete quantitative surface evaluation of four different methods. We used surface models derived from CT scans as a reference for the surface models obtained by surface scanning and photogrammetry. We also included landmark data captured by Microscribe digitizer because this has been a very common method of data collection in anthropology and comparative morphology. Deviations between professional surface scanners have been shown to be small (Kovacs et al., 2006; Kusnoto & Evans, 2002). Therefore, we decided to include only one surface scanner in this study and to focus on the quickly evolving field of photogrammetry by including various photogrammetric software.

Some studies showed that photogrammetry has low measurement error but did not address problems occurring during complex scanning processes (e.g., Fourie et al., 2011; Katz & Friess, 2014; Weinberg et al., 2006). Furthermore, many earlier studies were based on simple geometric objects or bones with relatively simple geometry, such as long bones (Bertsatos & Chovalopoulou, 2019; Hassett & Lewis-Bale, 2017; Marzke et al., 2010). We, therefore, applied these scanning methods to the human pelvis, which is intensively studied in current anthropology and evolutionary anatomy. As one of the most complex bones in the human skeleton, it combines various difficult areas for surface scanners and photogrammetry, such as holes, small gaps, thin crests and flat surfaces and thus allowed us to evaluate the limitations of the different methods.

7 | MATERIAL & METHODS

We created 3D surface models of four articulated human pelvises using photogrammetry, 3D surface scanning, and CT scanning. The pelvises are part of an Early Bronze Age (2200–1600 BC) skeletal collection excavated in Hainburg-Teichtal, Lower Austria, during the 1920s (Beninger et al., 1930) and curated in the Natural History Museum in Vienna (Inventory Nos. 6026, 9723, 12,134, 12,141). Two pelvises were female (age at death: 20–25 years and 30–39 years) and two were male (25–30 years and 35–45 years). They were only minimally taphonomically damaged and glued together in the 1970s. Four pelvises that were glued in the anatomical position were chosen in this study.

After an extensive search of different photogrammetric software packages, we included software based on the following inclusion criteria: the software must be suited for the photogrammetric evaluation of objects, it must still be supported and maintained by the developers, and surface meshes must be exportable for further analysis. Furthermore, all software either was freeware or a free academic or test version was available, which allowed us to test software of

different price categories. We ended up with 13 different photogrammetric software tools, including programs from well-known producers as well as new producers (Table 1).

For photogrammetry we used a Nikon DSLR-camera D5300 equipped with an AF-P Nikkor 18–55 mm 1:3.5–5.6G lens and an Apple iPhone 6 for software that are implemented as an app. The AF-P Nikkor lens and the iPhone 6 camera lens are known to have relatively strong distortions. Distortions are weakest in the center of the lens, close to its optical axis, and strongest at the margin. Taking a medium focal length, as suggested by Linder (2016), and leaving space between the pelvis and the margin of the photo to avoid areas with strong distortion effects reduced this problem. We took all pictures with a resolution of 24 megapixels, an exposure time of 1/100, an ISO-value of 100, and a focal ratio of 4.8. Additionally, a diffuse LED ring flash device from the company Neewer helped to reduce shadows and to increase the photo quality. The pelvis was placed on both ischial spines. Beneath the sacrum, a block of HAMA adhesive

putty for photography was placed to tilt the pelvis slightly anteriorly (approximately to 20°), in order to provide the best view into the pelvic canal. We took approximately 110–120 pictures in six tiers around each object, which proved to be an optimal compromise between data size and mesh quality: One tier was directed horizontally to the object, the second obliquely in a 45° angle, and the third one in a steep angle at approximately 80°. A picture was taken approximately every 18°. Then the pelvis was placed upside down and we repeated the three tiers. For the 3D reconstruction, we used a computer with an Intel Core i5-3350P processor (3.1 GHz), 16 GB RAM, an AMD Radeon HD 7900 graphic chip, and Windows 10 Pro, 64-bit. If the surface meshes contained considerable visual deviations from the original pelvis, we repeated the photographic procedure two further times with different settings to avoid errors caused by low-quality photos.

We also obtained surfaces with a 3D structured light scanner (Breuckmann-Smartscan) from AICON 3D Systems (a field of view of 30 cm resulted in a maximum resolution of 100 µm). White stickers,

TABLE 1 Overview of all photogrammetric software tested (last access: October 2020)

Software	Version	Producer	Costs	Exported formats	Notes
123D Catch (app; closed down)	2018	Autodesk	Freeware	stl	Quality highly dependent on cell phone camera, not suited for measurements
3df-Zephyr-lite	3.3	3DFlow	149\$ + VAT	mtl, obj, ply, stl	Best realistic rendering of all software, problems to reconstruct large, uncolored, smooth surfaces
3DSOM Pro	5	CDSL Limited	995\$ + 20% maintenance fee	3ds, collada, obj, stl, x3d,	Crash to desktop while surface mesh was reconstructed from point cloud
ARC3D	2.2	VISICS group - KU Leuven	Freeware	iv, obj, openSG, VRML2	Large holes in the meshes, irregular warping of the surface, very bad results
Photo Modeler Standard	2018	Photo Modeler Technologies	995\$	3ds, 3 dm, csv, dxf, fbx, igs, kml, kmz, las, ma, obj, pts, txt, wrl	Problems to reconstruct the iliac blades
Photoscan Pro	1.3.2	Agisoft	180 \$	3ds, dae, dxf, fbx, kmz, obj, pdf, ply, stl, u3d, wrl	Iliac blades partially missing in the meshes, At many areas bubble like appearance of the surface structure
PHOV (closed down)	2017	XLAB	Freeware	obj	Failed (“Error: Please contact the developers”)
Reality Capture	2018	Capturing Reality	99€ for 3 months or 4000 € + 25% maintenance fee	amc, aoa, asf, bvh, c3d, dae, dxf, fbx, htr, obj, partList, ply, mcd, trc, xyz	Nvidia graphic chip needed. Error message during reconstruction
ReCap Photo	19.0.1.9	Autodesk	30\$ monthly or 300\$ year; free education license	fbx, obj, stl	Worked fine
Sure pro	2.3	Nframes GmbH	Free education license	cesium, collada, esri, osgb, obj, slpk	Software crashed every time; not suited for simple photographs
TGI3D Photoscan	1.36	Ocali, Inc.	999 \$	skp	Only suitable in combination with Google sketch up
Trnio (app)	2018	Trnio Inc.	2.99\$	obj	Quality highly dependent on cell phone camera, not suited for measurements
Vi3dim Recon	2.3	Vi3DIM	395\$	obj, ply	Reconstructions failed

so-called targets, placed on the rotation board helped to reconstruct the surface models. We followed the standard scanning protocols (acquisition, aligning, fusion, noise reduction, gap filling) and saved all surface data as .stl files (geometry-only stereolithographic files).

As a reference, we performed clinical CT scans at the Veterinary University of Vienna (SOMATOM Emotion 16-slice configuration; Siemens AG Medical Solutions, Erlangen, Germany). Technical settings were 140 kV and 100 mA, the slice thickness was 0.5 mm and the pixel size 0.6 mm × 0.6 mm. We segmented all slices in Amira 6.7, following the segmentation protocol of Spoor et al. (1993).

In the post-processing, we detected and cleaned errors and outliers in the meshes obtained by photogrammetry and 3D surface scanning in Geomagic Design X (3D-Systems, 2015) using the built-in mesh doctor. We aligned the resulting surface models with the models extracted from the CT scans in Amira 6.7 for a qualitative analysis and in Geomagic Design X 5.1.0 for quantitative analysis. We explored differences by the mesh deviation tool in Geomagic Design.

In addition to this surface comparison, we performed a geometric morphometric analysis of landmark sets collected on the different surfaces. One observer (LW) placed a set of 219 3D landmarks and semilandmarks in Amira 6.7 twice on the surfaces achieved by photogrammetry, surface scanning, and CT scanning (Figure 1 and Table 2). Only landmarks present on all specimens were used. In addition, we collected all landmarks twice by a MicroScribe digitizer G2X on the physical bones (calibrated to an accuracy of 0.23 mm; Revware, 2019). The landmarks were recorded with remote control operated by foot and saved in an Excel spreadsheet. We implemented the morphometric and statistical analysis in R version 3.4.2 (R Core Team, 2013) using Geomorph version 3.0.7 (D. C. Adams et al., 2018). All semilandmarks were slid along their corresponding curve to minimize the bending energy between each individual and the sample mean shape (Gunz et al., 2005; Gunz & Mitteroecker, 2013). Subsequently, they were standardized for differences in overall location, scale and orientation by a generalized Procrustes analysis (Mitteroecker & Gunz, 2009; Rohlf & Slice, 1990). The resulting shape

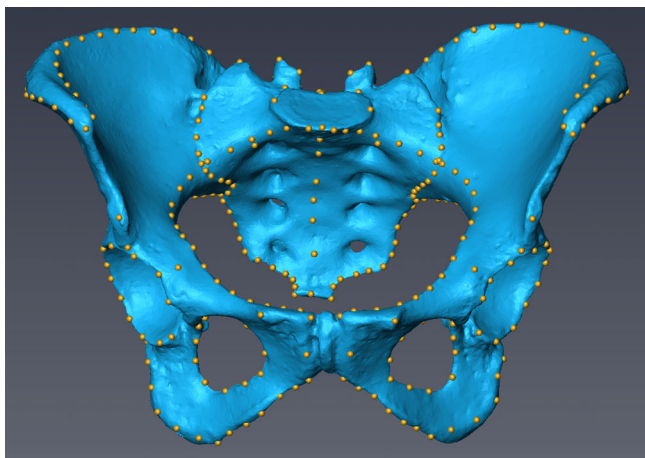


FIGURE 1 Landmarks placed on the surface mesh of an articulated pelvis (anterior–posterior view)

coordinates were explored by principal component analysis (PCA) to identify shape differences among the repeated measurements and between specimens.

8 | RESULTS

Most of the tested photogrammetric methods failed or rendered largely incomplete surface meshes of the articulated pelvis, which could not be reconstructed during the post-processing and therefore could not be included into a quantitative analysis (see Table 1). Two software (123D catch app and PHOV) had to be excluded from the study as they were already removed from the market. 3DSOM Pro, Reality Capture, Vi3dim Recon, and Sure Pro failed in the mesh

TABLE 2 Anatomical positions of all landmarks placed

Unpaired landmarks	Paired landmarks	Semilandmarks (no. of landmarks)
Promontory	Lateral point of S1 body	Alar-auricular ridge curvature (19)
S1 Center	Lateral alar-auricular point	Obturator foramen (23)
Third sacral segment union point	Inferior sacro-iliac junction	Acetabulum curvature (20)
Fourth sacral segment union point	Superior articular facet: medial superior corner	Pelvic inlet curvature (38)
Sacral canal, anterior floor	Superior articular facet: medial inferior corner	Greater sciatic notch curvature (18)
Sacral canal, anterior roof	Superior articular facet: lateral inferior corner	Ischial tuberosity curvature (18)
Sacral canal, posterior roof	Posterior superior iliospinale	Lateral iliac crest (38)
Dorsal spine of S1	Obturator tubercle point	Medial iliac crest (38)
Dorsal spine of S2	Superior anterior pubic symphysis	
	Superior posterior pubic symphysis	
	Pubotubercle point	
	Pubic eminence point	
	Anterior inferior iliospinale	
	Anterior acetabulum	
	Inferior acetabulum	
	Center point of acetabulum	
	Bouisson Tubercle point	
	Superior ischial tuberosity point	
	Ischiale	

calculation and showed error messages. The process was repeated two further times with different photos of different objects and failed every time. Sure Pro is probably only suited for aerial photogrammetry, though the producers mentioned it would also work for objects. Reality Capture only works in combination with an Nvidia graphic chip. We repeated the test sample on a suitable computer, but Reality Capture failed again. The failure of 3DSOM Pro was a surprise as this software is one of the most expensive programs used in this study (995\$ +199\$ maintenance fee per annum). Better results were obtained by 3df-Zephir-lite, which yielded a nicely rendered 3D surface, even though the iliac blades were missing. Agisoft Photoscan Pro showed considerable inaccuracies of both ilia and the pelvic canal.

An examination of the point clouds of all 3D models revealed that most software packages had troubles recognizing reference points on the flat surfaces of the iliac blades. The packages ARC3D and PHOV provided a complete surface model, but no feedback or possibilities to interfere with the single processing steps (aligning of photos, building the dense point cloud, building a 3D polygonal model, generating texture) were available. Similarly, the apps 123 catch and Trnio only implemented a surface mesh that could not be manipulated, even though errors in the surface meshes occurred quite often. Strong distortions of the cell phone lens as well as the small number of photos that could be handled by the cell phone hardware probably are the main reasons for these errors.

Only one software package, Autodesk Recap-photo, provided sufficient 3D surface information of the pelvis to continue with the topographical analysis. Autodesk Recap-photo contains two options for the surface mesh calculation: The surface mesh could be calculated on the owner's computer (but the minimum specifications are high: CPU of 2 GHz or faster, 64GB RAM, Nvidia GFX card with 4GB VRAM), or the photos are uploaded on the Autodesk server, where the surface mesh is computed (12\$ for up to 300 pictures). For research and education purposes up to 100 photos can be processed for free. One disadvantage of Autodesk Recap-photo was that no masking option was available in the software; photos had to be manipulated in Photoshop. However, masking did not provide better results in most cases since they were of high quality already. Only in case the photo stack visually produced a mesh of low quality, masking the background and repeating the mesh calculation lead to significantly better results in Autodesk Recap-photo. The surface calculation was automatic (e.g., exclusion of insufficiently aligned pictures and exclusion of outliers in the point cloud were not possible). In case the image set failed to provide sufficient information for the surface mesh, all pictures of the object had to be taken again, but this situation rarely occurred in our tests.

Comparing different conditions for the data collection revealed that an LED ring flash device was superior to a normal flash for avoiding shadows. This, in turn, reduced errors in the meshes. Completely closing the aperture of the camera helped to increase

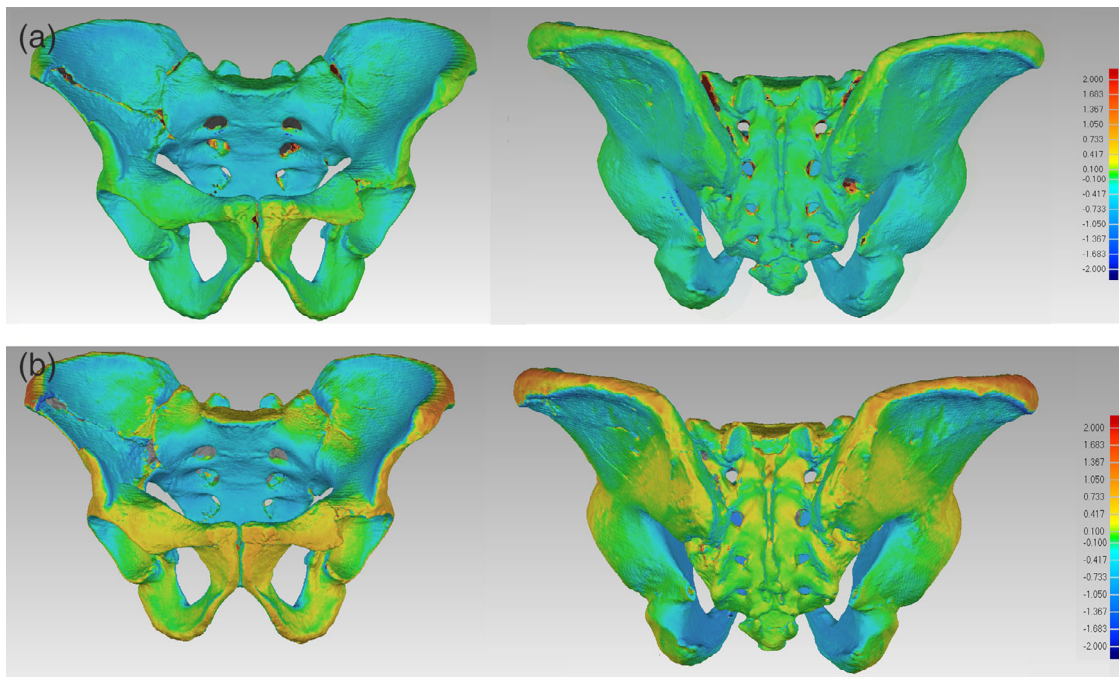


FIGURE 2 (a) Differences between the pelvic surfaces extracted from a clinical CT scan and photogrammetry, visualized as a color map. (b) Differences between the pelvic surfaces extracted from a clinical scan and 3D structured light scanner. A positive deviation indicates that the mesh obtained by surface scanning or photogrammetry is larger than the mesh obtained by CT scanning (yellow to red colored areas). In areas with a negative deviation, the photogrammetric or surface scanned mesh is smaller than the reference mesh of CT scanning (blue). If the surface differences were smaller than 100 μm, we defined these differences as non-relevant deviations between the methods. (green areas)

focus depth. A digital DSLR camera yielded better results in comparison to a mobile phone camera or a compact digital camera. DSLR cameras save image EXIF data (exposure time, focal ratio, focal distance, ISO, measurement mode, etc.), which can be read by various photogrammetric software and thus improves mesh calculation. Most photogrammetric software already have data about different cameras and objectives included. Many compact digital cameras do not save EXIF data with the photo file or estimate values by algorithms (e.g., iPhone).

Placing the object on a rotation board and fixing the camera on a tripod completely failed in all photogrammetric methods in this study if the photos were not masked. The option to define a permanent camera station (all pictures were taken from the same position, the object to scan was rotated), was only available in 3DSOM Pro, Photoscan Pro, and Vi3dim Recon. To avoid this, the background needs to be masked. Some photogrammetric software provides an in-built masking option (3df-Zephyr-lite, 3DSOM Pro, ARC3D, Photo Modeler Standard, Photoscan Pro). If this option is not available, the background needs to be masked with image manipulation software, such as Adobe Photoshop. Although the masking process can be done semi-automatically, lots of manual correction was needed for the pelvis, especially at shaded areas. For about 100 pictures per object, the manual correction was time-intensive (90 min per pelvis), but it

increased the quality of the surface mesh in various software (ARC3D, Photoscan Pro). Nevertheless, the quality of the surface meshes was visually still insufficient to continue a quantitative evaluation. Moreover, editing photos can lead to a loss of EXIF data, if the photos are saved as new files, and some photogrammetric software need the original, non-manipulated pictures (3df-Zephyr-lite, Photo Modeler Standard, Photoscan Pro, Sure pro), which makes masking and cropping in Photoshop impossible. In 123D catch app, masking was not possible, and the import of manipulated pictures also failed. The app Trnio implemented a rough automatic masking. Hence, the tested apps only worked if the pictures were taken directly with the apps.

All surface-generating methods had problems scanning articulated pelvises: many areas were difficult to access, for instance, the gaps in-between the ilia and the sacrum next to the sacroiliac joints and the dorsal side of the pubica. Other problematic structures were thin crests, such as the outline of the obturator foramen. In general, round objects or objects with flat and unicolored surfaces were difficult to scan.

In an initial qualitative analysis, surface data collected by CT, photogrammetry (using Autodesk Recap-photo) and 3D surface scanner were superimposed in the software Amira and visually compared. Sections through these surfaces showed minor differences between the surface models. Even small anatomical structures were present in all

	Photogrammetry versus CT	3D-structure-light- scanner versus CT	Photogrammetry versus 3D-structure-light- scanner
Minimum	-11.330	-14.242	-9.510
Maximum	10.584	12.992	9.836
Mean	0.168	0.164	0.107
Mean elevation	0.748	0.907	0.282
Mean depression	-1.135	-2.859	-0.235
Standard deviation	1.420	1.983	0.58
First quartile	-0.202	-0.225	-0.213
Second quartile	-0.163	-0.065	0.005
Third quartile	-0.139	0.135	0.101

TABLE 3 Descriptive statistics of average height differences [in mm] between the meshes obtained by different methods

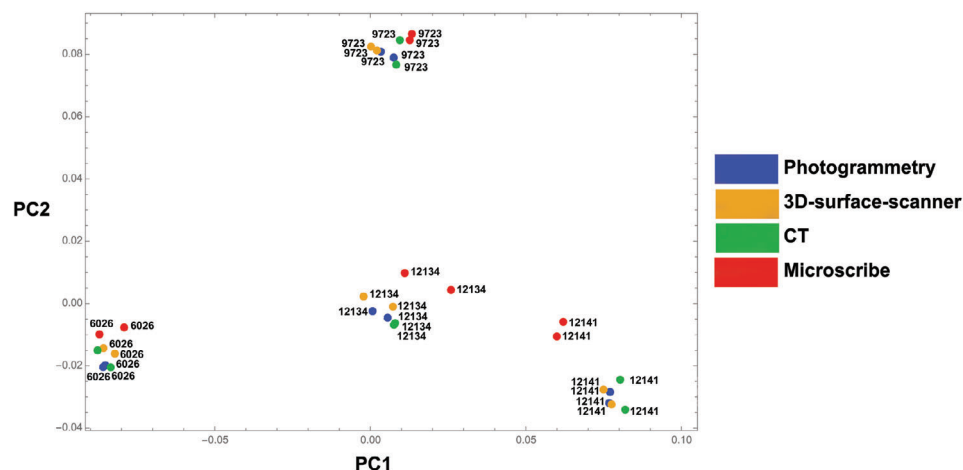


FIGURE 3 Principal component analysis (PCA). The first two PCs account for 67% of the total shape variance. The colors of the dots represent the scanning methods and the labels indicate the four different specimens

models. CT was the only method that provided accurate data of areas that are difficult to access with surface scanning methods, such as the sacral foramina, the sacral canal, and areas close to the sacroiliac joints. The topographical analysis showed minor differences of the iliac pillars, the dorsal sacrum, the inferior pubic rami and the acetabula across the scanning methods. Interestingly, in the photogrammetric models the dorsal pelvic surfaces were oriented slightly more inferiorly, toward the pelvic canal, whereas in the models obtained by 3D structured light scanner the ventral pelvic surface was more extended in comparison to CT scanning (Figure 2). Table 3 presents the average divergence of the surface meshes between CT scanning and photogrammetry or surface scanning. Mean elevation and depression refer to the average deviation of areas in the photogrammetric or surface scanned meshes, which are larger or smaller than the reference mesh, respectively. Maximal deviations between aligned surfaces cannot be interpreted well because they mostly correspond to holes in the meshes or misalignments. Quartiles are more meaningful in this context.

The PCA of the landmark shape coordinates showed that measurements of the same specimen clustered together (Figure 3). Landmark configurations of the same specimen (different surface meshes as well as repeated measurements) were more similar in shape than the differences between specimens, even though the landmarks obtained by the MicroScribe digitizer were slightly off the clusters for two specimens. Also, for this large set of 219 landmarks, some of the pelvises had to be measured multiple times with the MicroScribe because landmarks were forgotten or measured in the wrong order.

9 | DISCUSSION

Photogrammetry is increasingly used in anthropological research, and many new software packages have been released in recent years. With a large choice of software for photogrammetry in every price range, products need to be tested prior to the research application. Free or cheap software is not necessarily of poor quality. Photogrammetric software is constantly refined, and certain software that failed in this study might be suitable in updated versions. Only one software that we tested, Autodesk Recap-photo, was able to provide complete and accurate 3D surface models of the pelvises. Other tested photogrammetry software yielded partial models of the pelvises but failed to represent the iliac blades and thin crests. This software may thus still be able to provide accurate surface models of simple bones, such as long bones, or isolated pelvic bones (see below). Photogrammetry of one pelvis required a similar total work time as CT scanning (approximately 1 hr), but for CT scanning the material needed to be transported to the CT scanner. However, an efficient and reliable application of photogrammetry requires some training and experience.

The surface models yielded by the 3D surface scanner were similar to those obtained by photogrammetry but also captured the size of objects. However, 3D surface scanners are relatively large, expensive and may require special training. Both photogrammetry and surface

scanning require many overlapping photos or scans. For the Breuckmann scanner that we used in this study, a maximum of 30–40 scans from different angles were possible until the memory of the computer reached its full capacity (16 GB). Scanning the structure without the texture reduces the amount of data. Additionally, the automatic alignment of different surface scans often failed and had to be performed manually, which is time-consuming. On average, a surface scan with a complete representation of all areas of the articulated pelvis required 2 hr whereas photogrammetry photos of one pelvis were taken in 15–30 min. Depending on the photogrammetric software, masking of the background can increase the quality of the surface mesh (e.g., Photoscan Pro), which adds further 90 minutes to the working process of photogrammetry. Similarly, if tools are available to clean errors in the alignment of pictures, point cloud or mesh, the usage can increase the quality of the surface mesh. However, some programs need a certain graphic chip (e.g., Reality capture and the offline version of Recap Photo only work with an Nvidia graphic chip).

In order to assess if the computer hardware limited the success of photogrammetry, we monitored computer parameters during the mesh calculation. The stack of raw photos required approximately 1 GB of memory space (ca. 10 MB per photo). During the mesh calculations, photogrammetric software occupied up to 9 GB RAM. However, it might be possible that the computer allocated only a part of the available RAM to the photogrammetric software, causing the crash of some software when more RAM was needed. We therefore repeated all the mesh calculations on a more powerful computer (Intel Core i7-7700K 4.5 GHz, 64GB RAM, Geforce GTX 1080 graphic chip, Windows 10 Pro, 64-bit), but the results were the same. Software that crashed on the weaker computer also failed on the high-end computer, suggesting that the software failures were not caused by the hardware. In some software (e.g., Photoscan Pro), such incorrectly aligned images can be manually excluded from further processing, whereas problems in the calculation cannot be identified in completely automatic algorithms. We thus recommend to use photogrammetric software that allows insights into all steps of mesh calculation (masking, photo alignment, deletion of outliers in the dense point cloud, etc.) in research. However, Recap Photo showed that automatic algorithms can also provide precise models with low effort.

Recap photo contains an interesting option to outsource the mesh calculation to a server. Although the mesh processing cannot be manipulated, this software provides a quick option to achieve nicely rendered surface meshes without a powerful computer. However, we want to point out that uploading data of human remains to a company's server and giving them out of hands might be ethically problematic and not suited for all objects, for example, forensic material. Autodesk affirms that the users keep all rights on their data and that they are not used by Autodesk or passed to thirds.

Some software, such as 3DSOM Pro, 3df-Zephyr-lite and TGI3D Photoscan only provide a test version with limited options or had a limit for the maximal number of photos (Recap Photo). This might have had an impact on the results too as errors in the point clouds, or wrongly aligned pictures could not be identified. Hence, we cannot rule out that fully licensed software would have performed better

than the test versions. Cell phone apps are less suited for scientific purposes as the photo quality is usually much worse than a DSLR camera and cell phone hardware cannot match up to computer hardware. Compact cameras might work well for simpler objects, even though lens distortions usually are larger than lenses of professional cameras.

The results of the topographical analysis showed that CT scanning, 3D surface scanning and photogrammetry yielded similar surface models. Differences between surface models obtained by surface scanners and surface models extracted from CT scans were similar to those described in previous publications, albeit slightly smaller (e.g., Adams et al., 2015; Grant et al., 2019). The pelvic canal and iliac fossae were slightly larger in the photogrammetric and 3D surface scanner meshes as compared to the CT scan. The ventral pubica as well as iliac crests and anterior iliac spines were more strongly extended in the 3D surface scanner as compared to photogrammetry. Surface models obtained by the Breuckmann scanner had more problems in the pelvic canal and the obturator foramen in comparison to photogrammetry. We also had the opportunity to test a smaller, hand-hold 3D surface scanner on a cast of an articulated pelvis (Artec Eva, maximal resolution of 0.1 mm). Areas within the pelvic canal were easier to reach with the Artec Eva, as this scanner is smaller than the Breuckmann scanner and it is easier to scan the pelvic canal from the right angles. Nevertheless, scanning the sharp crest of the obturator foramen and the dorsal sides of the pubica were also problematic with the Artec Eva.

One cause of the differences among CTs, photogrammetry and 3D surface scanning was the difference in resolution. In this study, the maximum resolution of a clinical CT was 600 μm voxel size. Photogrammetry and surface scanning provided much better resolutions of approximately 100 μm . However, CT scans also provide accurate data of covered surfaces. A complete quantitative evaluation of the entire meshes is therefore difficult to interpret. The accuracy of photogrammetry and 3D surface scanning also depends on the shape of the object. An articulated human pelvis has a complex form. Large flat surfaces, thin crests and areas that are difficult to access might be the major reason why so many photogrammetric software failed. We also performed an additional test of a single coxal bone and a sacrum with the photogrammetric software used in this study. Indeed, single bone yielded better, though still not ideal results. Nonetheless, the narrow pelvic canal brought all surface scanning methods to their limits, which likely is one reason why so many photogrammetric software failed in this study. Additionally, we recognized that some photogrammetric software hardly found reference points at the smooth, curved and sometimes unicolored iliac blades. This affects the density of the point cloud at the iliac fossa. 3df-Zyphyr-lite produced a nicely rendered surface model of the pelvis but eliminated both iliac fossae from the mesh. Generally, for scanning smooth surfaces a professional structured light scanner is preferable. Scanning the iliac blades with the Breuckmann scanner was less problematic, although Recap Photo also provided comparable results easily. In summary, a professional surface scanner does not provide any additional advantage over photogrammetry but shows several disadvantages (heavy, expensive, training needed). All objects suited for a surface scanner can also be processed by photogrammetry. Only if the internal structure of an object is of interest, a CT scanner is necessary.

Acquiring data of articulated pelvis is difficult: In dry bone material, the joint surfaces usually do not match perfectly due to missing cartilage. Glued pelvis, as used in this study, are better suited for a methodological comparison of surface scanning and photogrammetry as the scanning results do not depend on the quality of the bone articulation with rubber strings. However, we are aware that gluing bones is often inappropriate for biological research as it may harm the objects and lead to imprecise fixation. Alternatively, isolated pelvic bones can be scanned and articulated virtually, but this is time-intensive and requires considerable experience due to the lack of haptic feedback. For one pelvis, we virtually articulated photogrammetric meshes of the isolated bones (landmark-based alignment as well as completely manual alignment) and found that it was difficult to precisely align both coxae and the sacrum in a reproducibly manner. We recommend a virtual articulation only for single cases but not for data collection of hundreds of cases, especially as error rates of virtual articulation have, to our knowledge, never been assessed.

We applied photogrammetry and the software Autodesk Recap-photo also for other, simpler objects, for example, a juvenile cranium and several experimentally produced pottery vessels. All these surfaces required fewer pictures, the masking of the background was easier and faster, and less post-processing was needed in comparison with the articulated pelvis. Bones with a relatively simple geometry, for instance long bones or vertebrae, and structures with more variation in surface texture (e.g., tuberosities on the diaphysis with a slightly different coloration and structure, tubercles, articulation surfaces, etc.) might thus be easier to assess by photogrammetry. Interestingly, the cranium was also relatively easy to scan despite the large unicolored curved bones; maybe the sutures were sufficient as reference points. Therefore, our results are not representative of all bones of the human skeleton. For bones with a simpler geometry, photo alignment can be performed more easily and requires less hardware resources.

Surface scanners and photogrammetry are also sensitive to light conditions. Surface scanners need a dark area for the scanning process as they illuminate the object with a projected grid on the object, whereas photogrammetry requires a well-lightened area for the object of interest. Using a photographic studio with several soft boxes provides the best results for photogrammetry, but such perfect laboratory conditions are unrealistic for anthropological data collection as human bones are usually stored in museums or osteological collections, which are often insufficiently lightened and do not provide the space necessary to set up a photographic studio. This combination of non-optimal light conditions and the complex geometry of the articulated human pelvis might be the main reasons why so many photogrammetric software failed in this study, although other researchers showed that precise surface meshes are possible (González et al., 2015; Rüter et al., 2012).

The PCA showed a clustering of all landmark configurations between the four different pelvis. Hence, all four methods provided relatively similar shape data, which is in agreement with previous studies (Friess, 2010, Sholts et al., 2010 in Friess, 2012, Munoz-Munoz 2016, Evin et al., 2016), even though landmarks captured by

TABLE 4 Comparison of important properties of photogrammetry, 3D surface scanning, CT scanning, and MicroScribe digitizer

	Photogrammetry	3D surface scanning	Clinical CT scanning	MicroScribe digitizer
Type of information	Surface (triangulated point cloud)	Surface (triangulated point cloud)	Volume (voxel)	3D coordinates of landmarks
Texture available	Yes	Yes (light-scanners only)	No	No
Maximum resolution (in μm)	100	20	500 (ca. 5 for micro-CT)	300
Total work time	1 h (+3 h of passive computer processing time)	5.5 h	1 h	30–45 min
Work time of subtasks	Photographs: 15 min Passive computer processing time to calculate a surface mesh: 3 h Post processing: 10 min Landmark placement: 30 min	Scanning time: 2 h Post processing: 3 h Landmark placement: 30 min	Scanning time: 2 min Post processing: 30 min Landmark placement: 30 min	Landmark placement: 30–45 min. For approx. 100 landmarks
Transportation	Portable	Portable	Samples need to be taken to the scanner	Portable
Scaling of the model	Not scaled	Scaled	Scaled	Scaled
Challenges	Reflective surfaces, small holes, sharp edges, translucent material	Hair, reflective surfaces, small holes, sharp edges, translucent material, dark colors	Metal, living individuals may be harmed, partial volume effect	Landmark placement requires physical object, might harm the object, difficult to check and correct measurements

the MicroScribe digitizer deviated most from the other landmark configurations. Setting landmarks on virtual surfaces by appropriate software allows one to edit the positions and order of landmarks. Furthermore, the surfaces and the measured landmarks can be assessed at any time, which allows one to show and discuss landmark positions and to add further landmarks. This greatly facilitates data collection and sharing. All of that this not possible with a MicroScribe digitizer. For our large landmark set, data collection with the MicroScribe digitizer was most prone to measurement error, including errors in the order and number of landmarks. In the course of our data collection, we had to repeat the recording of the entire landmark set several specimens. In such a case, access to the original objects is necessary, which may not be possible if the errors become evident only during the analysis. Measurements by a MicroScribe digitizer can also be influenced by the stylus placement and position of the joints of the sensor arm (Robinson & Terhune, 2017; Stephen et al., 2015) and thus require some experience with this tool (Sholts et al., 2011). A summary of all the compared methods is given in Table 4.

We recommend that researchers perform a small pilot study prior to a large data collection in order to test the usability of their material for photogrammetry and to test different photo parameters to achieve the best quality under the given scanning conditions.

ACKNOWLEDGMENTS

We thank the staff of the Department of Anthropology at the Natural History Museum in Vienna, in particular Margit Berner and Karin Wiltschke-Schrotta, who facilitated many aspects of our research, and Sophie Beitel for her feedback on the manuscript. Access to the

skeletons from Hainburg-Teichtal which are currently being prepared for publication, was granted by Alexandra Krenn-Leeb and Michaela Spannagl-Steiner.

This study was undertaken within the ERC-funded project “The value of mothers to society: responses to motherhood and child rearing practices in prehistoric Europe.” This project has received funding from the European Research Council (ERC) under the European Union's Horizon 2020 research and innovation programme (grant agreement No 676828).

CONFLICT OF INTEREST

The authors do not have a conflict of interest to declare.

AUTHOR CONTRIBUTIONS

Lukas Waltenberger: Conceptualization; data curation; formal analysis; investigation; methodology; writing-original draft. **Katharina Rebay-Salisbury:** Data curation; funding acquisition; project administration; supervision; writing-review and editing. **Philipp Mitteroecker:** Conceptualization; data curation; formal analysis; investigation; methodology; supervision; validation; writing-review and editing.

DATA AVAILABILITY STATEMENT

The data used in this study are available from the corresponding author upon request.

ORCID

Lukas Waltenberger  <https://orcid.org/0000-0002-9670-6117>

REFERENCES

- 3D-Systems. (2015). *Geomagic design X*. 3D Systems.
- Adams, D. C., Collyer, M. L., & Kaliontzopoulou, A. (2018). Geomorph: Software for geometric morphometric analyses. R package version 3.0.6 (Version 3.2.0).
- Adams, J. W., Olah, A., McCurry, M. R., & Potze, S. (2015). Surface model and tomographic archive of fossil primate and other mammal holotype and paratype specimens of the Ditsong National Museum of Natural History, Pretoria, South Africa. *PLoS One*, 10(10), 1–14. <https://doi.org/10.1371/journal.pone.0139800>.
- Aldridge, K., Boyadjiev, S. A., Capone, G. T., DeLeon, V. B., & Richtsmeier, J. T. (2005). Precision and error of three-dimensional phenotypic measures acquired from 3dMD photogrammetric images. *American Journal of Medical Genetics*, 138A, 247–253.
- Algee-Hewitt, B. F. B., & Wheat, A. D. (2016). Brief communication: The reality of virtual anthropology: Comparing digitizer and laser scan data collection methods for the quantitative assessment of the cranium. *American Journal of Physical Anthropology*, 160, 148–155. <https://doi.org/10.1002/ajpa.22932>.
- Aung, S. C., Ngim, R. C., & Lee, S. T. (1995). Evaluation of the laser scanner as a surface measuring tool and its accuracy compared with direct facial anthropometric measurements. *British Journal of Plastic Surgery*, 48, 551–558. [https://doi.org/10.1016/0007-1226\(95\)90043-8](https://doi.org/10.1016/0007-1226(95)90043-8).
- Beninger, E., Mühlhofer, F., & Geyer, E. (1930). Das frühbronzezeitliche Reihengräberfeld bei Hainburg-Teichtal. *Mitteilungen der Anthropologischen Gesellschaft in Wien*, 60, 65–142.
- Bertsatos, A., & Chovalopoulou, M.-E. (2019). A novel method for analyzing long bone diaphyseal cross-sectional geometry. A GNU octave CSG toolkit. *Forensic Science International*, 297, 65–71. <https://doi.org/10.1016/j.forsciint.2019.01.041>.
- Boldt, F., Weinzierl, C., Hertrich, K., & Hirschfelder, U. (2009). Comparison of the spatial landmark scatter of various 3D digitalization methods. *Journal of Orofacial Orthopedics*, 70(3), 247–263. <https://doi.org/10.1007/s00056-009-0902-2>.
- Bouby, L., Figueiral, I., Bouchette, A., Rovira, N., Ivorra, S., Lacombe, T., Pastor, T., Picq, S., Marinval, P., & Terral, J.-F. (2013). Bioarchaeological insights into the process of domestication of grapevine (*Vitis vinifera* L.) during Roman Times in southern France. *PLoS One*, 8(5), e63195. <https://doi.org/10.1371/journal.pone.0063195>.
- Breuer, T., Robbins, M. M., & Boesch, C. (2007). Using photogrammetry and color scoring to assess sexual dimorphism in wild Western Gorillas (*Gorilla gorilla*). *American Journal of Physical Anthropology*, 134, 369–382. <https://doi.org/10.1002/ajpa.20678>.
- Cardini, A., & Elton, S. (2008). Does the skull carry a phylogenetic signal? Evolution and modularity in the guenons. *Biological Journal of the Linnean Society*, 93(4), 813–834. <https://doi.org/10.1111/j.1095-8312.2008.01011.x>.
- Chen, H., Lowe, A. A., Strauss, A. M., de Almeida, F. R., Ueda, H., Fleeetham, J. A., & Wang, B. (2008). Dental changes evaluated with a 3D computer-assisted model analysis after long-term tongue retaining device wear in OSA patients. *Sleep and Breathing*, 12, 169–178. <https://doi.org/10.1007/s11325-007-0141-y>.
- Coquerelle, M., Prados-Frutos, J. C., Rojo, R., Mitteroecker, P., & Bastir, M. (2013). Short faces, big tongues: Developmental origin of the human chin. *PLoS One*, 8(11), e81287. <https://doi.org/10.1371/journal.pone.0081287>.
- Counts, D. B., Averett, E. W., & Garstki, K. (2016). A fragmented past: (re) constructing antiquity through 3D artefact modelling and customised structured light scanning at Athienou-Malloura, Cyprus. *Antiquity*, 90, 206–218. <https://doi.org/10.15184/aqy.2015.181>.
- Da Silveira, A. C., Daw, J. L., Kusnoto, B., Evans, C., & Cohen, M. (2003). Craniofacial applications of three-dimensional laser surface scanning. *Journal of Craniofacial Surgery*, 14, 449–456. <https://doi.org/10.1097/00001665-200307000-00009>.
- Dastane, A., Vaidyanathan, T. K., Vaidyanathan, J., Mehra, R., & Hesby, R. (1996). Development and evaluation of a new 3-D digitization and computer graphic system to study the anatomic tissue and restoration surfaces. *Journal of Oral Rehabilitation*, 23, 25–34. <https://doi.org/10.1111/j.1365-2842.1996.tb00808.x>.
- Evin, A., Souter, T., Hulme-Beaman, A., Ameen, C., Allen, R., Viacava, P., ... Dobne, K. (2016). The use of close-range photogrammetry in zooarchaeology: Creating accurate 3D models of wolf crania to study dog domestication. *Journal of Archaeological Science*, 9, 87–93. <https://doi.org/10.1016/j.jasrep.2016.06.028>.
- Faig, W. (1981). Close-range precision photogrammetry for industrial purposes. *Photogrammetria*, 36, 183–191. [https://doi.org/10.1016/0031-8663\(81\)90014-4](https://doi.org/10.1016/0031-8663(81)90014-4).
- Fourie, Z., Damstra, J., Gerrits, P. O., & Ren, Y. (2011). Evaluation of anthropometric accuracy and reliability using different three-dimensional scanning systems. *Forensic Science International*, 207(1–3), 127–134. <https://doi.org/10.1016/j.forsciint.2010.09.018>.
- Friess, M. (2010). Calvarial shape variation among Middle Pleistocene hominins: An application of surface scanning in palaeoanthropology. *Comptes Rendus Palevol*, 9(6–7), 435–443. <https://doi.org/10.1016/j.crpv.2010.07.016>.
- Friess, M. (2012). Scratching the surface? The use of surface scanning in physical and paleoanthropology. *Journal of Anthropological Sciences*, 90, 1–26. <https://doi.org/10.4436/jass.90004>.
- Geoghegan, B. (1953). The determination of body measurements, surface area and body volume by photography. *American Journal of Physical Anthropology*, 11, 97–120. <https://doi.org/10.1002/ajpa.1330110118>.
- Ghoddousi, H., Edler, R., Haers, P., Wertheim, D., & Greenhill, D. (2007). Comparison of three methods of facial measurement. *International Journal of Maxillofacial Surgery*, 36, 250–258. <https://doi.org/10.1016/j.ijom.2006.10.001>.
- Godin, G., Beraldin, A., Taylor, J., Cournoyer, L., Rioux, M., Hakim, S., ... Picard, M. (2002). Active optical 3D imaging for heritage applications. *IEEE Computer Graphics and Applications*, 22(5), 24–34. <https://doi.org/10.1109/MCG.2002.1028724>.
- González, M. A. M., Yravedra, J., González-Aguilera, D., Palomeque-González, J. F., & Domínguez-Rodrigo, M. (2015). Micro-photogrammetric characterization of cut marks on bones. *Journal of Archaeological Science*, 62, 128–142. <https://doi.org/10.1016/j.jas.2015.08.006>.
- Grant, C. A., Johnston, M., Adam, C. J., & Little, J. P. (2019). Accuracy of 3D surface scanners for clinical torso and spinal deformity assessment. *Medical Engineering & Physics*, 63, 63–71. <https://doi.org/10.1016/j.medengphy.2018.11.004>.
- Grosman, L., Smikt, O., & Smilansky, U. (2008). On the application of 3-D scanning technology for the documentation and typology of lithic artefacts. *Journal of Archaeological Science*, 35, 3101–3110. <https://doi.org/10.1016/j.jas.2008.06.011>.
- Gunz, P., & Mitteroecker, P. (2013). Semilandmarks: A method for quantifying curves and surfaces. *Hystrix*, 24(1), 103–109. <https://doi.org/10.4404/hystrix-24.1-6292>.
- Gunz, P., Mitteroecker, P., & Bookstein, F. L. (2005). Semilandmarks in three dimensions. In D. E. Slice (Ed.), *Modern morphometrics in physical anthropology* (pp. 73–98). Plenum.
- Hassett, B. R., & Lewis-Bale, T. (2017). Comparison of 3D landmark and 3D dense cloud approaches to hominin mandible morphometrics using structure-from-motion. *Archaeometry*, 59(1), 191–203. <https://doi.org/10.1111/arcm.12229>.
- Haukaas, C., & Hoddgetts, L. M. (2016). The untapped potential of low-cost photogrammetry in community-based archaeology: A case study from Banks Island, Arctic Canada. *Journal of Community Archaeology and Heritage*, 3, 40–56. <https://doi.org/10.1080/20518196.2015.1123884>.
- Hennessy, R. J., & Stringer, C. B. (2002). Geometric morphometric study of the regional variation of modern human craniofacial form. *American*

- Journal of Physical Anthropology*, 117, 37–48. <https://doi.org/10.1002/ajpa.10005>.
- Heritage, G. L., Fuller, I. C., Charlton, M. E., Brewer, P. A., & Passmore, D. P. (1998). CDW photogrammetry of low relief fluvial features: Accuracy and implications for reach-scale sediment budgeting. *Earth Surface Processes and Landforms*, 23(13), 1219–1233. [https://doi.org/10.1002/\(SICI\)1096-9837\(199812\)23:13<1219::AID-ESP927>3.0.CO;2-R](https://doi.org/10.1002/(SICI)1096-9837(199812)23:13<1219::AID-ESP927>3.0.CO;2-R).
- Hoffmann, E. J., Huang, S.-C., & Phelps, M. E. (1979). Quantitation in positron emission computed tomography: 1. Effect of object size. *Journal of Computer Assisted Tomography*, 3(3), 299–308. <https://doi.org/10.1097/00004728-197906000-00001>.
- Jaquet, N. (2006). A simple photogrammetric method to measure sperm whales at sea. *Marine Mammal Science*, 22, 862–879. <https://doi.org/10.1111/j.1748-7692.2006.00060.x>.
- Jayaratne, Y. S. N., Lo, J., Zwahlen, R. A., & Cheung, L. K. (2009). Three-dimensional photogrammetry or surgical planning of tissue expansion in hemifacial microsomia. *Head & Neck*, 32(12), 1728–1735. <https://doi.org/10.1002/hed.21258>.
- Katz, D., & Friess, M. (2014). Technical note: 3D from standard digital photography of human crania—a preliminary assessment. *American Journal of Physical Anthropology*, 154, 152–158. <https://doi.org/10.1002/ajpa.22468>.
- Kau, C. H., Richmond, S., Zhurov, A. I., Knox, J., Chestnutt, I., Hartles, F., & Playle, R. (2005). Reliability of measuring facial morphology with a 3-dimensional laser scanning system. *American Journal of Orthodontics and Dentofacial Orthopedics*, 128(4), 424–439. <https://doi.org/10.1016/j.ajodo.2004.06.037>.
- Kovacs, L., Zimmermann, A., Brockmann, G., Guhring, M., Baurecht, H., Papadopulos, N. A., ... Zeilhofer, H. F. (2006). Three-dimensional recording of the human face with a 3D laser scanner. *Journal of Plastic Reconstructive and Aesthetic Surgery*, 59, 1193–1202. <https://doi.org/10.1016/j.bjps.2005.10.025>.
- Kraus, K. (2007). *Photogrammetry—Geometry from images and laser scans* (2nd ed.). Walter de Gruyter GmbH.
- Kusnoto, B., & Evans, C. A. (2002). Reliability of a 3D surface laser scanner for orthodontic applications. *American Journal of Orthodontics and Dentofacial Orthopedics*, 122, 342–348. <https://doi.org/10.1067/mod.2002.128219>.
- Kuzminsky, S., & Gardiner, M. (2012). Three-dimensional laser scanning: Potential uses for museum conservation and scientific research. *Journal of Archaeological Science*, 39(8), 2744–2751. <https://doi.org/10.1016/j.jas.2012.04.020>.
- Lane, S. N., Richards, K. S., & Chandler, J. H. (1996). Discharge and sediment supply controls on erosion and deposition in a dynamic alluvial channel. *Geomorphology*, 15(1), 1–15. [https://doi.org/10.1016/0169-555X\(95\)00113-J](https://doi.org/10.1016/0169-555X(95)00113-J).
- Lichti, D., Gordon, S. J., Stewart, M. P., Franke, J., & Tsakiri, M. (2002). Comparison of Digital Photogrammetry and Laser Scanning. *Proceedings CIPA WG 6 International Workshop on Scanning Cultural Heritage Recording, Corfu, Greece, 1–2 September 2002*, 39–44.
- Linder, W. (2016). *Digital photogrammetry - a practical course* (4th ed.). Springer-Verlag.
- Littlefield, T. R., Kelly, K. M., Cherney, J. C., Beals, S. P., & Pomatto, J. K. (2004). Technical strategies: Development of a new three-dimensional cranial imaging system. *Journal of Craniofacial Surgery*, 15, 175–181. <https://doi.org/10.1097/00001665-200401000-00042>.
- Lloyd, M. S., Buchanan, E. P., & Khechoyan, D. Y. (2016). Review of quantitative outcome analysis of cranial morphology in craniosynostosis. *Journal of Plastic, Reconstructive & Aesthetic Surgery*, 69(11), 1464–1468. <https://doi.org/10.1016/j.bjps.2016.08.006>.
- Loy, A., Tamburelli, A., Carlini, R., & Slice, D. E. (2011). Craniometric variation of some Mediterranean and Atlantic populations of *Stenella coeruleoalba* (Mammalia, Delphinidae): A three-dimensional geometric morphometric analysis. *Marine Mammal Science*, 27(2), E65–E78. <https://doi.org/10.1111/j.1748-7692.2010.00431.x>.
- Marcus, J. R., Domeshek, L. F., Das, R., Marshall, S., Nightingale, R., Stokes, T. H., & Mukundan, S., Jr. (2008). Objective three-dimensional analysis of cranial morphology. *Eplasty*, 8, e20.
- Marmulla, R., Hassfeld, S., Luth, T., & Muhling, J. (2003). Laser-scan-based navigation in craniomaxillofacial surgery. *Journal of Cranio-Maxillo-Facial Surgery*, 31, 267–277. [https://doi.org/10.1016/s1010-5182\(03\)00056-8](https://doi.org/10.1016/s1010-5182(03)00056-8).
- Martin, R., & Knußmann, R. (1988). *Anthropologie: Handbuch der vergleichenden Biologie des Menschen*. Gustav Fischer Verlag.
- Marzke, M. W., Tocheri, M. W., Steinberg, B., Femiani, J. D., Reece, S. P., Linscheid, R. L., Orr, C. M., & Marzke, R. F. (2010). Comparative 3D quantitative analyses of trapeziometacarpal joint surface curvatures among living catarrhines and fossil hominins. *American Journal of Physical Anthropology*, 141(1), 38–51. <https://doi.org/10.1002/ajpa.21112>.
- Mehta, B. V., & Marinescu, R. (2001). *Comparison of Image Generation And Processing Techniques For 3D Reconstruction of The Human Skull*. Paper presented at the 23rd Annual EMBS International Conference, Istanbul, Turkey.
- Menéndez, L. P. (2016). Comparing methods to assess intraobserver measurement error of 3D craniofacial landmarks using geometric morphometrics through a digitizer arm. *Journal of Forensic Sciences*, 62(3), 741–746. <https://doi.org/10.1111/1556-4029.13301>.
- Metscher, B. D. (2009). MicroCT for developmental biology: A versatile tool for high-contrast 3D imaging at histological resolutions. *Developmental Dynamics*, 238(3), 632–640. <https://doi.org/10.1002/dvdy.21857>.
- Milne, N., Vizcaíno, S. F., & Fernicola, J. C. (2009). A 3D geometric morphometric analysis of digging ability in the extant and fossil cingulate humerus. *Journal of Zoology*, 278(1), 48–56. <https://doi.org/10.1111/j.1469-7998.2008.00548.x>.
- Mitteroecker, P., & Gunz, P. (2009). Advances in geometric morphometrics. *Evolutionary Biology*, 36, 235–247. <https://doi.org/10.1007/s11692-009-9055-x>.
- Mitteroecker, P., Gunz, P., Bernhard, M., Schaefer, K., & Bookstein, F. L. (2004). Comparison of cranial ontogenetic trajectories among great apes and humans. *Journal of Human Evolution*, 46(6), 679–697. <https://doi.org/10.1016/j.jhevol.2004.03.006>.
- Motani, R. (2005). Detailed tooth morphology in a durophagous ichthyosaur captured by 3D laser scanner. *Journal of Vertebrate Paleontology*, 25, 462–465. [https://doi.org/10.1671/0272-4634\(2005\)025\[0462:DTMIAD\]2.0.CO;2](https://doi.org/10.1671/0272-4634(2005)025[0462:DTMIAD]2.0.CO;2).
- Munoz-Munoz, F., Quinto-Sanchez, M., & Gonzales-Jose, R. (2016). Photogrammetry: A useful tool for three dimensional morphometric analysis of small mammals. *Journal of Zoological Systematics and Evolutionary Research*, 54(4), 318–325. <https://doi.org/10.1111/jzs.12137>.
- Neubauer, S., Gunz, P., Scott, N. A., Hublin, J. J., & Mitteroecker, P. (2020). Evolution of brain lateralization: A shared hominid pattern of endocranial asymmetry is much more variable in humans than in great apes. *Science Advances*, 6(7), eaax9935. <https://doi.org/10.1126/sciadv.aax9935>.
- Niven, L., Steele, T. E., Finke, H., Gernat, T., & Hublin, J.-J. (2009). Virtual skeletons: Using a structured light scanner to create a 3D faunal comparative collection. *Journal of Archaeological Science*, 36, 2018–2023. <https://doi.org/10.1016/j.jas.2009.05.021>.
- Nunez, M. A., Buill, F., & Edo, M. (2013). 3D model of the Can Sadurní cave. *Journal of Archaeological Science*, 40, 4420–4428. <https://doi.org/10.1016/j.jas.2013.07.006>.
- O'Higgins, P., & Jones, N. (1998). Facial growth in *Cercocebus torquatus*: An application of three-dimensional geometric morphometric techniques to the study of morphological variation. *Journal of Anatomy*, 193, 251–272. <https://doi.org/10.1046/j.1469-7580.1998.19320251.x>.

- Owen, J., Dobney, K., Evin, A., Cucchi, T., Larson, G., & Vidarsdottir, U. S. (2014). The zooarchaeological application of quantifying cranial shape differences in wild boar and domestic pigs (*Sus scrofa*) using 3D geometric morphometrics. *Journal of Archaeological Science*, 43, 159–167. <https://doi.org/10.1016/j.jas.2013.12.010>.
- Plooi, J. M., Swennen, G. R. J., Rangel, F. A., Maal, T. J., Schutyser, F. A., Bronkhorst, E. M., Kuijpers-Jagtman, A. M., & Bergé, S. J. (2009). Evaluation of reproducibility and reliability of 3D soft tissue analysis using 3D stereophotogrammetry. *International Journal of Oral Maxillofacial Surgery*, 38(267–273), 267–273. <https://doi.org/10.1016/j.ijom.2008.12.009>.
- Porter, S. T., Roussel, M., & Soressi, M. (2016). A simple photogrammetry rig for the reliable creation of 3D artefact models in the field lithic examples from the early upper Paleolithic sequence of Les Cottés (France). *Advances in Archaeological Practice*, 4, 71–86. <https://doi.org/10.7183/2326-3768.4.1.71>.
- R Core Team. (2013). *R: A language and environment for statistical computing*. R Foundation for Statistical Computing.
- Revware. (2019). MicroScribe G2 Specifications sheet. Retrieved from http://www.revware.net/wp-content/uploads/2012/05/7_MicroScribe_G_Product_Brochure.pdf
- Robinson, C., & Terhune, C. E. (2017). Error in geometric morphometric data collection: Combining data from multiple sources. *American Journal of Physical Anthropology*, 164(1), 62–75. <https://doi.org/10.1002/ajpa.23257>.
- Rohlf, F. J., & Slice, D. E. (1990). Extensions of the Procrustes method for the optimal superimposition of landmarks. *Systematic Zoology*, 39(1), 40–59. <https://doi.org/10.2307/2992207>.
- Ross, A. H., & Williams, S. (2008). Testing repeatability and error of coordinate landmark data acquired from crania. *Journal of Forensic Sciences*, 53, 782–785. <https://doi.org/10.1111/j.1556-4029.2008.00751.x>.
- Rüther, H., Smit, J., & Kamamba, D. (2012). A comparison of close-range photogrammetry to terrestrial laser scanning for Heritage documentation. *South African Journal of Geomatics*, 1(2), 149–162.
- Rutty, G. N., Brough, A., Biggs, M. J. P., Robinson, C., Lawes, S. D. A., & Hainsworth, S. V. (2013). The role of micro-computed tomography in forensic investigations. *Forensic Science International*, 225(1–3), 60–66. <https://doi.org/10.1016/j.forsciint.2012.10.030>.
- Sapirstein, P. (2016). Accurate measurement with photogrammetry at large sites. *Journal of Archaeological Science*, 66, 137–145. <https://doi.org/10.1016/j.jas.2016.01.002>.
- Sholts, S. B., Flores, L., Walker, P. L., & Wärländer, S. K. T. S. (2011). Comparison of coordinate measurement precision of different landmark types on human crania using a 3D laser scanner and a 3D digitizer: Implications for applications of digital morphometrics. *International Journal of Osteoarchaeology*, 21, 535–543. <https://doi.org/10.1002/oa.1156>.
- Sholts, S. B., Wärländer, S. K. T. S., Flores, L. M., Miller, K. W. P., & Walker, P. L. (2010). Variation in the measurement of cranial volume and surface area using 3D laser scanning technology. *Forensic Science International*, 55(4), 871–876. <https://doi.org/10.1111/j.1556-4029.2010.01380.x>.
- Shrader, A. M., Ferreira, S. M., & van Aarde, R. J. (2006). Digital photogrammetry and laser rangefinder techniques to measure African elephants. *South African Journal of Wildlife Research*, 36, 1–7.
- Singleton, M. (2002). Patterns of cranial shape variation in the Papionini (Primates: Cercopithecinae). *Journal of Human Evolution*, 42(5), 547–578. <https://doi.org/10.1006/jhev.2001.0539>.
- Spoor, C. F., Zonneveld, F. W., & Macho, G. A. (1993). Linear measurements of cortical bone and dental enamel by computed tomography: Applications and problems. *American Journal of Physical Anthropology*, 91, 469–484. <https://doi.org/10.1002/ajpa.1330910405>.
- Stephen, A. J., Wegscheider, P. K., Nelson, A. J., & Diceky, J. P. (2015). Quantifying the precision and accuracy of the MicroScribe G2X three-dimensional digitizer. *Digital Applications in Archaeology and Cultural Heritage* 2, 2(1), 28–33. <https://doi.org/10.1016/j.daach.2015.03.002>.
- Tocheri, M. W., Razdan, A. R., Williams, C., & Marzke, M. W. (2005). A 3D quantitative comparison of trapezium and trapezoid relative articular and nonarticular surface area in modern humans and great apes. *Journal of Human Evolution*, 49(5), 570–586. <https://doi.org/10.1016/j.jhev.2005.06.005>.
- Toma, A. M., Zhurov, A., Playle, R., Ong, E., & Richmond, S. (2009). Reproducibility of facial soft tissue landmarks on 3D laser-scanned facial images. *Orthodontics and Craniofacial Research*, 12(1), 33–42. <https://doi.org/10.1111/j.1601-6343.2008.01435.x>.
- Van Vlijmen, O. J. C., Rangel, F. A., Bergé, S. J., Bronkhorst, E. M., Becking, A. G., & Kuijpers-Jagtman, A. M. (2011). Measurements on 3D models of human skulls derived from two different cone beam CT scanners. *Journal of Clinical Oral Investigations*, 15, 721–727. <https://doi.org/10.1007/s00784-010-0440-8>.
- Verhoeven, G., Doneus, M., Briese, C., & Vermeulen, F. (2012). Mapping by matching: A computer vision-based approach to fast and accurate georeferencing of archaeological aerial photographs. *Journal of Archaeological Science*, 39, 2060–2070. <https://doi.org/10.1016/j.jas.2012.02.022>.
- Vidarsdottir, U. S., O'Higgins, P., & Stringer, C. (2002). The development of regionally distinct facial morphologies: A geometric morphometric study of population-specific differences in the growth of the modern human facial skeleton. *Journal of Anatomy*, 201, 211–229. <https://doi.org/10.1046/j.1469-7580.2002.00092.x>.
- Von Cramon-Taubadel, N., Frazier, B. C., & Lahr, M. M. (2007). The problem of assessing landmark error in geometric morphometrics: Theory, methods and modifications. *American Journal of Physical Anthropology*, 134, 24–35. <https://doi.org/10.1002/ajpa.20616>.
- Vu, A. F., Chundury, R. V., & Perry, J. D. (2017). Comparison of the FaroArm laser scanner with the MicroScribe digitizer using Basicranial measurements. *The Journal of Craniofacial Surgery*, 28(5), e460–e463. <https://doi.org/10.1097/SCS.00000000000003741>.
- Wachowiak, M., & Karas, B. (2009). 3D scanning and replication for museum and cultural heritage applications. *Journal of the American Institute for Conservation*, 48(2), 141–158. <https://doi.org/10.1179/019713609804516992>.
- Weinberg, S. M., Naidoo, S., Govier, D. P., Martin, R. A., Kane, A. A., & Marazita, M. L. (2006). Anthropometric precision and accuracy of digital three-dimensional photogrammetry: Comparing the Genex and 3dMD imaging systems with one another and with direct anthropometry. *Journal of Craniofacial Surgery*, 17, 477–483. <https://doi.org/10.1097/00001665-200605000-00015>.
- Windhager, S., Mitteroecker, P., Rupi, I., Lauc, T., Polašek, O., & Schaefer, K. (2019). Facial aging trajectories: A common shape pattern in male and female faces is disrupted after menopause. *American Journal of Physical Anthropology*, 169(4), 678–688. <https://doi.org/10.1002/ajpa.23878>.
- Yamada, T., Mori, Y., Minami, K., Mishima, K., & Tsukamoto, Y. (2002). Three-dimensional analysis of facial morphology in normal Japanese children as control data for cleft surgery. *Cleft Palate Craniofacial Journal*, 39, 517–526. https://doi.org/10.1597/1545-1569_2002_039_0517_tdaofm_2.0.co_2.

How to cite this article: Waltenberger L, Rebay-Salisbury K, Mitteroecker P. Three-dimensional surface scanning methods in osteology: A topographical and geometric morphometric comparison. *Am J Phys Anthropol*. 2021;174:846–858. <https://doi.org/10.1002/ajpa.24204>